Multidimensional Systems and Signal Processing, 14, 119–137, 2003

Signal Processing for Large Bandwidth and Long Duration Waveform SAR

ZHIPING LIN[1] ezplin@ntu.edu.sg
School of EEE, Nanyang Technological University, Singapore

YONGHONG ZENG eyhzeng@ntu.edu.sg
School of EEE, Nanyang Technological University, Singapore
National University of Defense Technology, P.R. China

GUOAN BI egbi@ntu.edu.sg
School of EEE, Nanyang Technological University, Singapore

JOCELYN YEO
DSO National Laboratories, Singapore

Received April 11, 2001; Revised September 28, 2001; Accepted December 7, 2001

Abstract. We first show that for some kinds of signals a "bandwidth and time duration reduction technique" can be used to simulate waveform distortions caused by moving targets, that is, it is correct to measure the waveform distortions at very large TB with relatively small v by reducing TB and increasing v while keeping TBv unchanged, where T is the duration of the transmitted signal, B is the bandwidth and v is the relative speed of targets. We then study the waveform distortions in SAR signals caused by moving antenna. Based on the bandwidth and time duration reduction technique, a lot of time and memory are saved in simulations. We then confirm by simulations that waveform distortions do pose problems when processing very large bandwidth and long duration SAR data using conventional SAR processing methods. Finally we propose the concepts of wideband and narrowband processing of SAR data. Models are set up for wideband and narrowband SAR data processing, and new methods are presented for reconstructing targets using the proposed models. Simulations show that the methods can improve the quality of the simulated SAR images.

Key Words: large bandwidth, long duration waveform, SAR data processing, SAR model, SAR image

1. Introduction

The common mode of operation for conventional SAR is like this: while an aircraft carrying a SAR sensor is flying along a particular path, an antenna transmits a short duration waveform (pulse), then receives an echo corresponding to this pulse, transmits another pulse and so on. Due to the motion of antenna, relative motion of targets during transmission and reception of a pulse always exists. This relative motion causes distortions (dilations) in the received waveforms. In conventional SAR, since the pulse duration is very short, this distortion can be ignored. This makes traditional SAR signal processing relatively easy and explains the fact that currently most (if not all) practical SAR systems use very short pulses as their waveforms for transmission [13]. On the other hand, using large bandwidth and long duration waveforms do have some advantages. First, low

probability of interception (LPI) may be achieved. It is relatively easy for an intercept receiver to detect the radiated signal of conventional radars at long ranges [1], [10], [19]. To reduce a radar's detectability to a hostile intercept receiver, its peak power should be made as low as possible. The radiated energy should be spread over a wide angular, over a long time interval, and over a wide frequency band [12]. So, if a SAR system can transmit a long duration waveform, the instantaneous power of the transmitted signal will be reduced and LPI be achieved. Second, large bandwidth and long duration waveform leads to large time-bandwidth product and may improve the resolution of SAR imaging [5], [14]. Ultra high carrier frequency waveform can be used to improve the cross-range resolution. The Twin-Otter SAR developed at the Sandia National Laboratories can operate on frequency band as high as in the Ka (14 to 16 GHz) and Ku (32.6 to 37 GHz) bands [15]. Its spotlight resolution can reach higher than 1 meter. The central carrier frequency of the currently used millimeter-wave radar can be larger than 10GHz [7], [9], [18]. Such kind of radars have been widely used in many areas [7], [9], [18]. We believe large bandwidth and ultra high carrier frequency could be used in future SAR systems.

For a SAR system with large bandwidth, ultra high carrier frequency and large time duration, the waveform distortion (dilation) due to relative motion of targets during transmission and reception of a pulse cannot be ignored anymore, especially when the speed of the platform is very high such as in spaceborne radar [3], [4], [6], [8]. Since traditional signal processing methods for SAR ignore such distortions, they may not be valid anymore here. There are many auto-focus and motion compensation algorithms [2], [13], [16]. However, since each of them has its own purpose and is based on its own conditions, they cannot be used for our case directly. For example, most known motion compensation algorithms have the following assumptions [2], [13] (for example, see [13], section 6.7, pp. 465–477): (a) the speed of the targets are constant; (b) the speed is so small that the targets can be treated as motionless during transmission and reception of a pulse. These two assumptions are obviously not valid in our case. In SAR, the relative speeds of targets with respect to the antenna are dependent on the location of the antenna and the location of the targets. In large bandwidth and long duration case, dilations in received SAR signal cannot be ignored based on our simulations. This means that targets cannot be treated as motionless during transmission and reception of a pulse. So the problem discussed by us is much more difficult and new methods must be proposed. The purpose of this paper is to investigate the waveform distortion in SAR and seek methods to improve the distorted images.

The rest of paper is organized as follows. We first propose a "bandwidth and time duration reduction technique" in section 2. In order to reduce the computational complexity for simulation purpose, we show that for some kinds of signals it is correct to measure waveform distortions for very large TB with relatively small υ by reducing TB and increasing υ while keeping $TB\upsilon$ unchanged, where and henceforth T is the duration of the transmitted signal, B is the bandwidth and υ is the relative speed of the target. We then study the waveform distortion due to the moving antenna in section 3. Simulations are done to show waveform distortions in very large bandwidth and long duration SAR data by using conventional SAR processing methods. The concepts of wideband and narrowband processing of SAR data are proposed in section 4. We present new methods for

reconstructing targets using the proposed models. Simulations show that the methods can improve the quality of the simulated SAR images.

2. Bandwidth and Time Duration Reduction Technique

2.1. Waveform Distortions Due to Moving Targets

It is well known that when a transmitter/receiver and an object (target) reflecting the transmitted waveform have relative motion, the received waveform will be distorted. The amount of distortion depends on the waveform, the relative motion and the speed of propagation of the signal [17]. Assume that the transmitted signal is $p(t)$ and the target is moving at a constant velocity v. It has been shown [17] that the echoed signal of a single point-target at distance R_0 (the distance of the target at time 0) is

$$s(t) = p(a(t - \tau)), \tag{1}$$

where

$$\tau = 2R_0/c, \ a = \frac{c - v}{c + v}, \tag{2}$$

and c is the speed of the light. When the transmitted signal is a narrowband signal, the time scaling can be further approximated by the Doppler shift. More accurately, if the "narrowband condition" [11], [17] is satisfied, that is,

$$TB \ \leq \ \frac{0.1c}{v}. \tag{3}$$

or

$$TBv \ \leq \ 0.1c, \tag{4}$$

the echoed signal can be approximated by

$$s(t) \approx p(t - \tau)e^{-j2\pi f_d}, \tag{5}$$

where $f_d = \frac{2v}{c} f_c$ is the Doppler frequency shift and f_c is the central carrier frequency. However, for wideband signals we have to consider the more general case of time scaling, that is, the time scaling (dilation) factor a must be considered and it should not be approximated by a Doppler shift.

2.2. Bandwidth and Time Duration Reduction Technique

Before carrying out actual simulations, it is noticed that for signals with large time bandwidth product, the amount of data to be processed will be huge. For wideband signal of frequency bandwidth B and time duration T, at least 2TB discrete samples are required

to represent the signal. If T $= 10^{-3}$ (s) and B $= 1000$ (MHz), at least 2 million samples are required! In SAR applications, we also need to sample the synthetic aperture domain. The number of samples depends on the size of the synthetic aperture, the radar frequency and the size of the cross range in the illuminated area. If 1000 samples are chosen in the synthetic aperture, we have totally 2×10^9 samples. This will require considerable amount of processing time as well as huge memory. In order to reduce the complexity for simulating the waveform distortion in SAR, we propose a "bandwidth and time duration reduction technique" in the following to simplify the simulation process.

It is observed that for certain waveforms such as chirps, the shape and properties of the waveforms will be preserved after the bandwidth of waveforms is reduced while the time duration keeps unchanged. Since the main concern here is waveform distortion, it suffices to show that waveform distortion remains unchanged for both signals with the original bandwidth and with a reduced bandwidth. Notice the factors causing waveform distortion are given in expression (3). Hence if the bandwidth B is reduced 10 times, and the velocity of aircraft is at the same time increase 10 times, condition (3) remains unchanged and the amount of waveform distortion, if any, will remain unchanged. We show this in the following when the transmitted signal is a chirp.

Let the transmitted signal be an up-chirp, $p(t) = e^{j\alpha t + j\beta t^2}$,where α is the carrier frequency and β is the chirp rate. When the speed of the target is υ, the received signal $s(t)$ is described in (1). If the target is stationary, the received signal is then $s_1(t) = p(t - \tau)$, where τ is the same as that in (1). For the investigation of waveform distortion, τ can be assumed to be 0. So, the difference between $s(t)$ and $s_1(t)$ is then

$$s(t) - s_1(t) = e^{ja\alpha t + ja^2\beta t^2} - e^{j\alpha t + j\beta t^2}. \tag{6}$$

Since $\upsilon \ll c$, we have $a = \frac{c-\upsilon}{c+\upsilon} \approx 1 - \frac{2\upsilon}{c}$. Furthermore, $a^2 \approx 1 - \frac{4\upsilon}{c}$. Therefore,

$$s(t) - s_1(t) \approx e^{j\alpha t + j\beta t^2}(e^{-j\frac{2\upsilon}{c}\alpha t - j\frac{4\upsilon}{c}\beta t^2} - 1). \tag{7}$$

$$|\, s(t) - s_1(t) \,| \approx |\, e^{-j\frac{2\upsilon}{c}\alpha t - j\frac{4\upsilon}{c}\beta t^2} - 1 \,|. \tag{8}$$

We know that the bandwidth B of the signal is approximately βT and the central carrier frequency is nearly $\alpha + \beta T/2$. If we keep the ratio of the bandwidth and carrier frequency to be constant, that is, the relative bandwidth $\frac{\beta T}{\alpha + \beta T/2}$ is a constant q, and also keep the product of the speed of the target and bandwidth, $B\upsilon$, to be constant, we know that the difference in (8) remains unchanged. In fact, since $\alpha = \left(\frac{1}{q} - \frac{1}{2}\right)\beta T = \left(\frac{1}{q} - \frac{1}{2}\right)B$ and $\beta\upsilon = \frac{B}{T}\upsilon$, (8) can be turned to

$$|\, s(t) - s_1(t) \,| \approx |\, e^{-j\frac{2B\upsilon}{c}\left(\frac{1}{q} - \frac{1}{2}\right)t - j\frac{4B\upsilon}{cT}t^2} - 1 \,|, \tag{9}$$

where $B\upsilon$, q and T are fixed. So, the difference is constant. That is, we can measure the waveform distortion by keeping $B\upsilon$ to be constant and allow B to be small while υ very large.

Table 1. Mean square error of the distorted signal (Chirp).

Bandwidth	Duration	Speed of targets	Error
20MHz	10μs	3000Km/s	1.4161
200MHz	10μs	300Km/s	1.4046
2GHz	10μs	30Km/s	1.4035
20GHz	10μs	3Km/s	1.4034
20MHz	100μs	300Km/s	1.4234
200MHz	100μs	30Km/s	1.4026
2GHz	100μs	3Km/s	1.4033
20GHz	100μs	300m/s	1.4140

Simulations are conducted to test this observation, and it works even when the bandwidth is reduced as much as 1000 times! There are some small deviations due to the finite data length effect, which are insignificant for the investigation on waveform distortion. For example, to investigate waveform distortion for a signal with bandwidth 20GHz, and the velocity of target being 300 m/s, it is equivalent to do the same for a signal with bandwidth 20MHz, and the velocity of target being 300 Km/s! Of course there is no aircraft in the real world can travel at such a high speed. But it works well if we just want to know the effect of time-bandwidth product on waveform distortion. We use the up-chirps for our simulations. The simulations result are listed in Table 1. In our simulations, the center carrier frequency is the same as the bandwidth, that is, $q = 1$. The table gives the mean square error of the distorted signal with respect to the undistorted signal ($\upsilon = 0$), that is,

$$\sqrt{\sum_i |s_1(t_i) - s(t_i)|^2} \Big/ \sqrt{\sum_i |s_1(t_i)|^2}. \tag{10}$$

We assume that we have one target at distance 2000 meters. As can be seen from Table 1, the relative errors caused by waveform distortions are significant and hence cannot be ignored.

This observation is also valid for step chirp signals. We can prove this theoretically similarly as we did for chirp before. For other signals, this observation must be checked carefully. A major problem is that for most other kinds of signals, bandwidths depend on time durations. That is, when the bandwidth increase the time duration usually must be shortened. For example, for a biphase signal, its bandwidth depends on the width of each subpulse, say T_s. If the time duration of the signal is fixed, say T, then to keep with the increase of the bandwidth, the number of subpulses, say N, must also increase so that the reciprocal of the width of each subpulse, N/T, is proportional to the increased bandwidth. When the bandwidth increase from B to $10B$, the number of subpulses must also increase form N to $10N$. However, in practice, in order to achieve good auto-correlation function only certain types of biphase signals are useful such as Barker code. If we use the Barker code, when the time duration of the signal T is fixed, the length-N Barker code is very different from the length-$10N$ Barker code since the Barker code is chosen randomly. So, how can we compare the distortions of the received signals if the transmitted signals

Table 2. Mean square error of the distorted signal (Frank code).

Bandwidth	Duration	Speed of targets	Error
20MHz	10μs	3000Km/s	1.4050
80MHz	10μs	750Km/s	1.4029
320Hz	10μs	187.5Km/s	1.3906
1.28GHz	10μs	46.875Km/s	1.3908

are very different? It is meaningless to compare the distortions on such cases. Furthermore, it is very difficult to get the Barker code for large number of subpulses. Frank code is easy to be used since we can easily produce any length Frank code. We have done some simulations on this code (see Table 2). Here we use the width of the mainlobe as the bandwidth of the signal. Therefore, if the time duration is fixed to be $10\mu s$, $20MHz$ bandwidth corresponds to $N = 100$ subpulses. For the step frequency code, such as Costas code, this observation also seems nearly correct. Table 3 gives the simulation results, where the length-24 Costas code is used.

Another observation is that for certain waveforms such as chirps, the impact of waveform distortion on the reconstructed image quality is almost unchanged if we fix B and the product $T\upsilon$ respectively while letting T and υ vary. We have done some simulations to support this observation in one-dimensional range radars. We assume the following scene. The transmitted signal is an up-chirp. There are four targets in the area. The distance of the center of targets is 2000m (meter) and all targets are located in $[2000 - 50, 2000 + 50]$ m. Three targets are at distance 2000m, 2035m and 1975m respectively, which are independent on the radar parameters. Another targets is at distance $2035 + 2 * dx$ m, where dx is the sampling interval in the range domain which depends on the bandwidth. The bandwidth and the central carrier frequency are 200MHz. In Figure 1-a, we assume that the targets are stationary and the time duration of transmitted signal is 10μs. In Figure 1-b to 1-d, we assume the speed of the targets is 300Km/s, 30Km/s and 3Km/s respectively, and the time duration of the signals are 10μs, 100μs and 1000μs respectively. From Figure 1-b to 1-d, we see that the images of the reconstructed targets are almost unchanged. So, for simulation purpose, in order to save time and memory, we can replace long time duration by high speed. For example, to investigate the impact of waveform distortion on the quality of reconstructed image when the time duration is 1000μs and the velocity of target is 3 Km/s, it is equivalent to do the same for a signal with time duration of 10μs and the velocity of target being 300 Km/s!

Table 3. Mean square error of the distorted signal (Costas code).

Bandwidth	Duration	Speed of targets	Error
20MHz	10μs	3000Km/s	1.3796
80MHz	10μs	750Km/s	1.4136
320Hz	10μs	187.5Km/s	1.4148
1.28GHz	10μs	46.875Km/s	1.4151

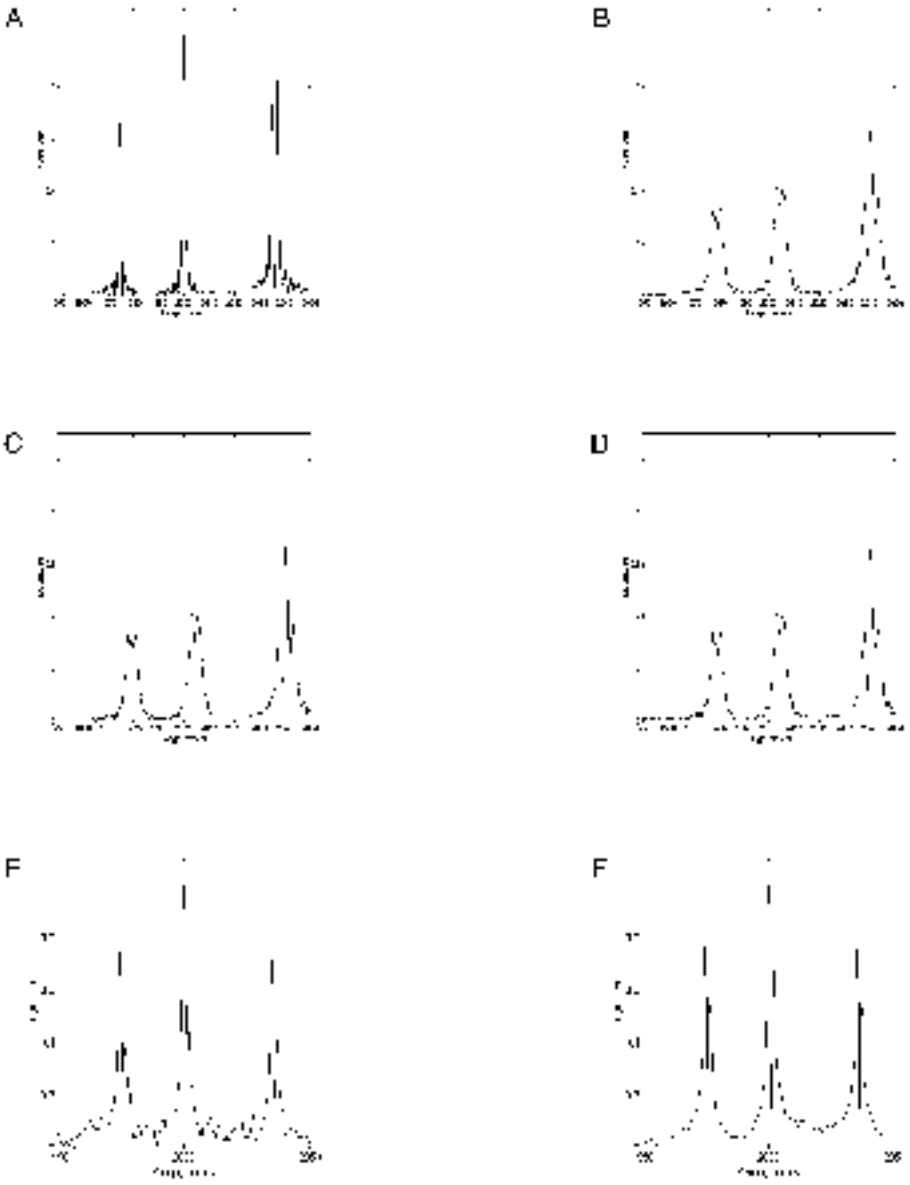

Figure 1. (a) Range reconstruction via matched filtering ($B = 200MHz$, $T = 10us$, $\upsilon = 0$). (b) Range reconstruction via matched filtering ($B = 200MHz$, $T = 10us$, $\upsilon = 300Km/s$). (c) Range reconstruction via matched filtering ($B = 200MHz$, $T = 100us$, $\upsilon = 30Km/s$). (d) Range reconstruction via matched filtering ($B = 200MHz$, $T = 1000us$, $\upsilon = 3Km/s$). (e) Range reconstruction via matched filtering (Frank code) ($B = 200MHz$, $T = 0.25us$, $\upsilon = 1200Km/s$). (f) Range reconstruction via matched filtering (Frank code) ($B = 200MHz$, $T = 16us$, $\upsilon = 18.75Km/s$).

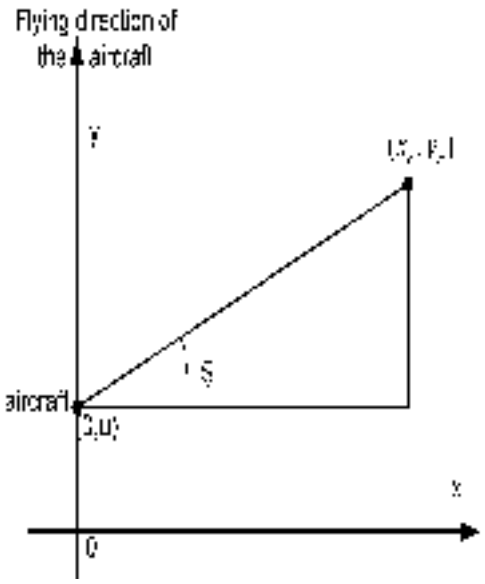

Figure 2. System Model for SAR.

This observation is also true for step chirp signal. For other types of signals, this observation must be checked carefully. For Frank code, this observation seems nearly correct. To keep the bandwidth unchanged, we keep the ratio N/T to be constant. In our simulations, the bandwidth is fixed at $200MHz$. When $T = 0.25\mu s$, N is chosen to be 5. Figures 1-*e* to 1-*f* are the simulation results.

In general, for some signals like chirps the impact of waveform distortion on the quality of reconstructed image is nearly unchanged if we keep $TB\upsilon$ constant while letting υ be very large and TB be relatively small. This bandwidth and time duration reduction technique will enable us to save a large amount of time and memory for simulations in large bandwidth and long duration SAR signal processing.

3. Waveform Distortion in SAR Due to Moving Antenna

For large bandwidth and ultra high carrier frequency SAR applications, the waveform distortion due to the moving antenna may not be ignored. We consider the following model for SAR [13]: the transmitted signal is $p(t)$, the aircraft is moving at a constant velocity υ, and the speed of propagation of the signal is c. The targets are located at (x_n, y_n) $(n = 1, 2, \cdots, N)$, where x_n is the slant-range and y_n is the cross-range (see Figure 2). For simplicity, all the targets are assumed motionless. The aircraft is flying along the y axis and its location is then $(0, u)$, where $u \in [-L, L]$. $2L$ is the length of synthetic aperture.

From Figure 2, we see that

$$\sin\theta_n = \frac{y_n - u}{\sqrt{x_n^2 + (y_n - u)^2}}. \tag{11}$$

The reflected signal by target (x_n, y_n) is then

$$s_n(t,u) = \sigma_n p(\lambda_n(t - \tau_n)), \tag{12}$$

where σ_n is the reflective coefficient of target (x_n, y_n),

$$\lambda_n = \frac{c + \upsilon \sin\theta_n}{c - \upsilon \sin\theta_n}, \tag{13}$$

$$\tau_n = 2\sqrt{x_n^2 + (y_n - u)^2}/c. \tag{14}$$

So, the received signal should be

$$s(t,u) = \sum_{n=1}^{N} s_n(t,u) = \sum_{n=1}^{N} \sigma_n p(\lambda_n(t - \tau_n)). \tag{15}$$

A major difference between the dilation λ_n here and the dilation a in one dimensional case in (1) is that λ_n not only depends on the speed υ but also on the direction of the target. This causes the wideband processing method for SAR which will be discussed in the following section much more difficult.

In current SAR practice, the scale factors λ_n are ignored, that is, the received signal is approximated by [13]

$$\bar{s}(t,u) = \sum_{n=1}^{N} \bar{s}_n(t,u) = \sum_{n=1}^{N} \sigma_n p(t - \tau_n). \tag{16}$$

We will show that such a simplification may lead to big errors sometimes when the bandwidth of the transmitted waveform is very large and the time duration of the waveform is long. We have done some simulations for spotlight SAR by using the wavefront reconstruction method and M. Soumekh's Matlab programs ([13], chapter 5, pp. 319–372) and the above received signal formulae (15) and (16). As discussed above, we know that the waveform distortion is determined by the time bandwidth product TB and the relative speed υ. Furthermore, based on the derivation in section 2, we know that for some waveforms such as chirps, the impact of waveform distortion on the reconstructed image remains almost unchanged if we keep $TB\upsilon$ constant while letting υ be very large and TB be relatively small. To save computational time, we would like TB to be as small as possible.

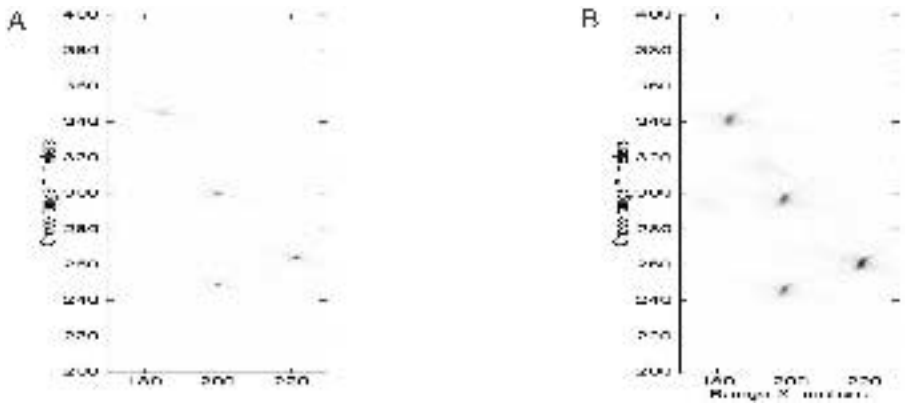

Figure 3. (a) Reconstructed SAR image ($B = 200MHz$, $T = 0.1us$, $\upsilon = 0$). (b) Reconstructed SAR image ($B = 200MHz$, $T = 0.1us$, $\upsilon = 40{,}000Km/s$).

So, in our simulations, we keep TB to be small while letting the speed υ be very large. This is of course not the case in practice. However, the results are almost the same when TB is very large while υ is relatively small. We give three examples in the following.

(I) For Figures 3-a to 3-b, the basic parameters are as follows:

$B = 200MHz$ (bandwidth)
$f_c = 200MHz$ (central carrier frequency)
$X_c = 200m$ (target center in slant range)
$X_0 = 30m$ ($2X_0$ is the length of slant range)
$Y_c = 300m$ (target center in cross range)
$Y_0 = 60m$ ($2Y_0$ is the length of cross range)
$L = 200m$, $T = 0.1\mu s$.

The results for $\upsilon = 0$, $\upsilon = 40{,}000Km/s$ are shown in the Figures 3-a to 3-b respectively. When $\upsilon = 40{,}000Km/s$, the $TB\upsilon$ is then 8×10^8 m/s. If we consider the ordinary speed for aircraft, that is, $\upsilon = 200m/s$, then, to keep the $TB\upsilon$ unchanged, we need TB to be 4×10^6. We can choose B to be $4GHz$ and T to be $1ms$, or other pairs of values for B and T. This is practical.

(II) For Figures 4-a to 4-b, the basic parameters are the same as those in Figure 3-a and Figure 3-b except that the speed of the aircraft is reduced to $\upsilon = 400Km/s$ and the time duration is raised to $T = 10\mu s$. The results for $\upsilon = 0$, $\upsilon = 400Km/s$ are shown in the Figures 4-a to 4-b respectively. It is clearly seen that the reconstructed image in Figure 4-b is of the same quality as that in Figure 3-b. The $TB\upsilon$ here is the same as that in the previous example. We can imagine that similar results occur when the aircraft flies at the ordinary speed, $\upsilon = 200m/s$, while the bandwidth B is $8GHz$ and T is 0.5ms. In spaceborne radar [3], [4], the speed can be as high as $\upsilon = 10Km/s$. Hence we can expect similar results occur

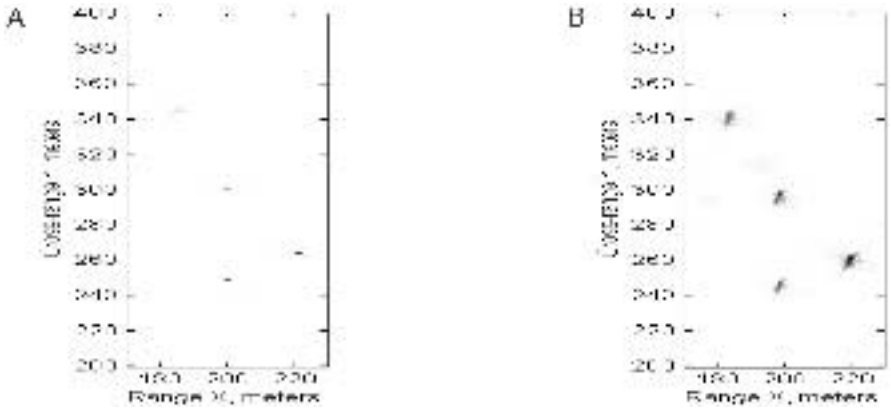

Figure 4. (a) Reconstructed SAR image ($B = 200MHz$, $T = 10us$, $\upsilon = 0$). (b) Reconstructed SAR image ($B = 200MHz$, $T = 10\mu s$, $\upsilon = 400Km/s$).

for spaceborne radar when $B = 800MHz$ and $T = 0.1ms$, which is reasonable in the near future.

(III) For Figures 5-a to 5-b, the basic parameters are as follows:

$B = 2GHz$, $f_c = 2GHz$, $X_c = 200m$, $X_0 = 20m$
$Y_c = 300m$, $Y_0 = 30m$, $L = 50m$, $T = 0.1\mu s$.

The results for $\upsilon = 0$, $\upsilon = 20{,}000Km/s$ are shown in the Figures 5-a to 5-b respectively. When $\upsilon = 20{,}000Km/s$, the $TB\upsilon$ is then 4×10^9 m/s. If we consider the ordinary speed for

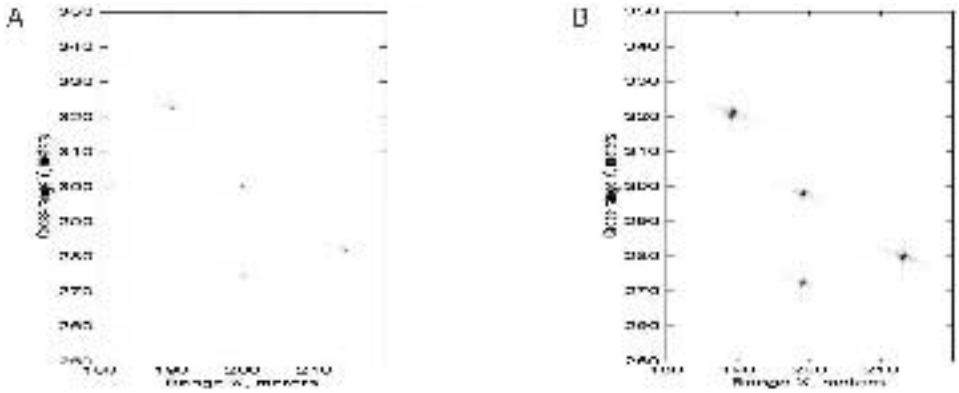

Figure 5. (a) Reconstructed SAR image ($B = 2GHz$, $T = 0.1\mu s$, $\upsilon = 0$). (b) Reconstructed SAR image ($B = 2GHz$, $T = 0.1\mu s$, $\upsilon = 20{,}000Km/s$).

aircraft, that is $\upsilon = 200m/s$, then, to keep the $TB\upsilon$ unchanged, we need TB to be 2×10^7. We can choose B to be $20GHz$ and T to be $1ms$, which are reasonable in SAR.

The simulations show that the waveform distortion cannot be ignored when the bandwidth of the transmitted waveform is very large and the time duration of the waveform is long. We should develop methods to deal with the problem.

4. Wideband and Narrowband Processing for SAR Signals

As discussed in the previous section, we need new methods to deal with the waveform distortion in SAR signals. Unlike ordinary range radars, SAR detect targets in two- or three-dimensional space. This leads to much higher complexity in signal processing algorithms for SAR signals. The wideband and narrowband processing methods for one-dimensional signals are no longer valid for SAR [11], [17]. Although there are many auto-focus and motion compensation algorithms, as explained in the introduction they cannot be used here directly. New methods should be proposed. In this section, based on the analysis of the received SAR signal, we will propose new methods for the problem. Like one-dimensional case, we call a method which considers the dilation of the received SAR signal a **wideband processing method** for SAR signals.

We now further analyze the received SAR signal. For $\upsilon \ll c$,we have

$$\lambda_n \approx 1 + \frac{2\upsilon}{c}\sin\theta_n,\ \frac{1}{\lambda_n} \approx 1 - \frac{2\upsilon}{c}\sin\theta_n. \tag{17}$$

So, by using (17) and the first order approximation in the Taylor series expansion, we have

$$\begin{aligned} s(t,u) &= \sum_{n=1}^{N} \sigma_n p(\lambda_n(t-\tau_n)) \\ &\approx \sum_{n=1}^{N} \sigma_n p\left[\left(1 + \frac{2\upsilon}{c}\sin\theta_n\right)(t-\tau_n)\right] \\ &\approx \sum_{n=1}^{N} \sigma_n p(t-\tau_n) + \sum_{n=1}^{N} \sigma_n p'(t-\tau_n)\frac{2\upsilon\sin\theta_n}{c}(t-\tau_n). \end{aligned} \tag{18}$$

Let $S(\omega, u)$ be the Fourier transform of $s(t, u)$ with respect to fast time t and $P(\omega)$ be the Fourier transform of $p(t)$. We get

$$\begin{aligned} S(\omega,u) &= \sum_{n=1}^{N} \sigma_n/\lambda_n P(\omega/\lambda_n)e^{-j\omega\tau_n} \\ &\approx \sum_{n=1}^{N} \sigma_n P(\omega/\lambda_n)e^{-j\omega\tau_n} \end{aligned}$$

$$\approx \sum_{n=1}^{N} \sigma_n P\left(\omega - \frac{2v\sin\theta_n}{c}\omega\right) e^{-j\omega\tau_n}$$

$$\approx \sum_{n=1}^{N} \sigma_n \left[P(\omega) - P'(\omega)\frac{2v}{c}\frac{y_n - u}{\sqrt{x_n^2 + (y_n - u)^2}}\omega\right] e^{-j\omega\tau_n}$$

$$\approx P(\omega)\sum_{n=1}^{N} \sigma_n e^{-j\omega 2\sqrt{x_n^2+(y_n-u)^2}/c}$$

$$-\omega P'(\omega)\sum_{n=1}^{N} \sigma_n \frac{2v}{c}\frac{y_n - u}{\sqrt{x_n^2 + (y_n - u)^2}} e^{-j\omega 2\sqrt{x_n^2+(y_n-u)^2}/c}. \tag{19}$$

Since the currently available methods (see [13], e.g.) for detecting targets (x_n, y_n) all ignore the last term in the equation (18) or (19), errors are inevitable. Suitable methods for compensating the impact of the term must be found.

Like narrowband processing in the one-dimensional case [6], [8], we can also replace the dilation by Doppler frequency shifts. However, in SAR the Doppler frequency shifts are not only related to the speed of the vehicle, but also related to the direction of the targets. This makes the problem much more difficult. When $TB \leq \frac{0.1c}{v}$, a **narrowband processing for SAR** signals is as follows.

Let f_d^n be the Doppler frequency shift, that is,

$$f_d^n = \frac{2v\sin\theta_n}{c} f_c, \tag{20}$$

where f_c is the central carrier frequency. If the narrowband condition (3) is satisfied, we have

$$s(t,u) \approx \sum_{n=1}^{N} \sigma_n p(t-\tau_n) e^{j2\pi f_d^n (t-\tau_n)}. \tag{21}$$

In frequency domain, we have,

$$S(\omega,u) \approx \sum_{n=1}^{N} \sigma_n P(\omega + 2\pi f_d^n) e^{-j\omega\tau_n}$$

$$\approx \sum_{n=1}^{N} \sigma_n P\left(\omega + \frac{4\pi v f_0}{c}\frac{y_n - u}{\sqrt{x_n^2 + (y_n - u)^2}}\right) e^{-j\omega 2\sqrt{x_n^2+(y_n-u)^2}/c}. \tag{22}$$

As discussed above, either wideband processing or narrowband processing for SAR signals is very different from that in the one-dimensional case. The known methods for the one-dimensional case (see [17], e.g.) cannot be used directly. In the following, we give two iterative methods which can be used to improve the quality of reconstructed SAR images.

From (16) and (18) we see that

$$\begin{aligned}\bar{s}(t,u) &= \sum_{n=1}^{N} \sigma_n p(t-\tau_n) \\ &= s(t,u) - \sum_{n=1}^{N} \sigma_n p'(t-\tau_n)\frac{2\upsilon \sin\theta_n}{c}(t-\tau_n). \end{aligned} \tag{23}$$

If we can get $\bar{s}(t, u)$, we can use the currently known methods such as the wavefront reconstruction method [13] to locate the targets (x_n, y_n) and find the reflective coefficient σ_n. In practice, what we get is the received signal $s(t, u)$. Due to the impact of the second term in (18), using known methods such as the wavefront reconstruction method on the received signal $s(t, u)$ cannot get images in good quality, which are shown in Figures 3–5. However, when we get a rough estimation of $(x_n, y_n)$and σ_n, we can use them to improve the quality of the image. If the rough estimation of the targets and the reflectivities are $(\tilde{x}_n, \tilde{y}_n)$ and $\tilde{\sigma}_n$ respectively $(n = 1, 2, \cdots, N)$, we get an approximation for $\bar{s}(t, u)$ by

$$\bar{s}(t,u) \approx s(t,u) - \sum_{n=1}^{N} \tilde{\sigma}_n p'(t-\tilde{\tau}_n)\frac{2\upsilon \sin\tilde{\theta}_n}{c}(t-\tilde{\tau}_n), \tag{24}$$

where

$$\sin\tilde{\theta}_n = \frac{\tilde{y}_n - u}{\sqrt{\tilde{x}_n^2 + (\tilde{y}_n - u)^2}}, \tag{25}$$

$$\tilde{\tau}_n = 2\sqrt{\tilde{x}_n^2 + (\tilde{y}_n - u)^2}/c. \tag{26}$$

We call this method "**Wideband Compensation**".

We have done simulations based on the above method. An example is shown below. We first use the wavefront reconstruction method [13] on the received signal $s(t, u)$ to get a rough image of the targets (Figure 4-b). From the rough image, we get an estimation of the location of the targets and the reflectivities. Then we use (24) to get an approximation for $\bar{s}(t, u)$. Finally, the wavefront reconstruction method is used again on $\bar{s}(t, u)$ to get an image (Figure 6-a). The process can be done iteratively until we get a satisfactory image. Simulations have shown that this method can improve the quality of the image. The radar parameters here are described in the example (I) of section 3. Figure 4-a is the reconstructed image when the speed of the aircraft $\upsilon = 0$. Figures 7-a to 7-c are the corresponding 3D images of Figure 4-a, Figure 4-b and Figure 6-a respectively, where the values are normalized so that they are in the interval [0,255]. The mean square error (MSE) between Figure 7-a and Figure 7-c is 0.0207. The mean square error (MSE) between Figure 7-a and Figure 7-b is 0.0398. So after one iteration, the MSE is reduced by nearly one half.

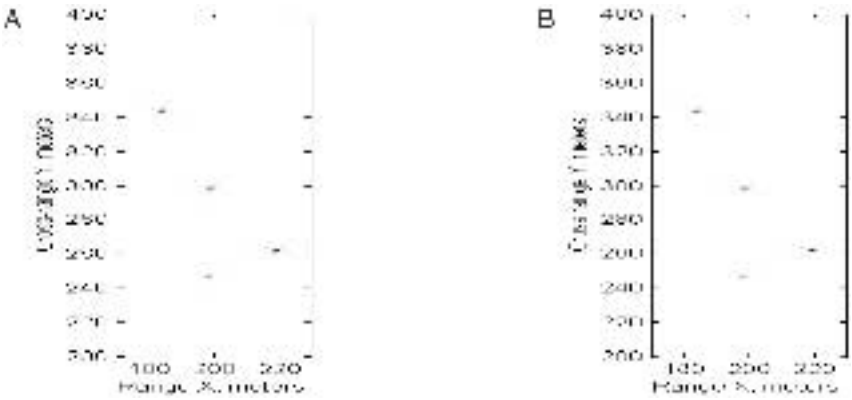

Figure 6. (a) Wideband compensation SAR image ($\upsilon = 400Km/s$). (b) Narrowband compensation SAR image ($\upsilon = 400Km/s$).

When the narrowband condition is satisfied, we can also improve the image quality using the approximation (21). Based on (21) and the first order approximation of the Taylor series expansion, we have

$$s(t,u) \approx \sum_{n=1}^{N} \sigma_n p(t-\tau_n) + \sum_{n=1}^{N} \sigma_n j2\pi f_d^n (t-\tau_n) p(t-\tau_n). \tag{27}$$

So,

$$\begin{aligned} \bar{s}(t,u) &= \sum_{n=1}^{N} \sigma_n p(t-\tau_n) \\ &\approx s(t,u) - \sum_{n=1}^{N} \sigma_n j2\pi f_d^n (t-\tau_n) p(t-\tau_n). \end{aligned} \tag{28}$$

As discussed above, we can use the wavefront reconstruction method to reconstruct the image if we have a good approximation of $\bar{s}(t, u)$. When we get a rough estimation of (x_n, y_n) and σ_n, we can use them to improve the quality of the image. If the rough estimation of the targets and the reflectivities are $(\tilde{x}_n, \tilde{y}_n)$and $\tilde{\sigma}_n$ respectively $(n = 1, 2, \cdots, N)$, we get an approximation for $\bar{s}(t, u)$ as

$$\bar{s}(t,u) \approx s(t,u) - \sum_{n=1}^{N} \tilde{\sigma}_n j2\pi \tilde{f}_d^n (t-\tau_n) p(t-\tilde{\tau}_n), \tag{29}$$

where

$$\tilde{f}_d^n = \frac{2\upsilon \sin\tilde{\theta}_n}{c} f_c, \tag{30}$$

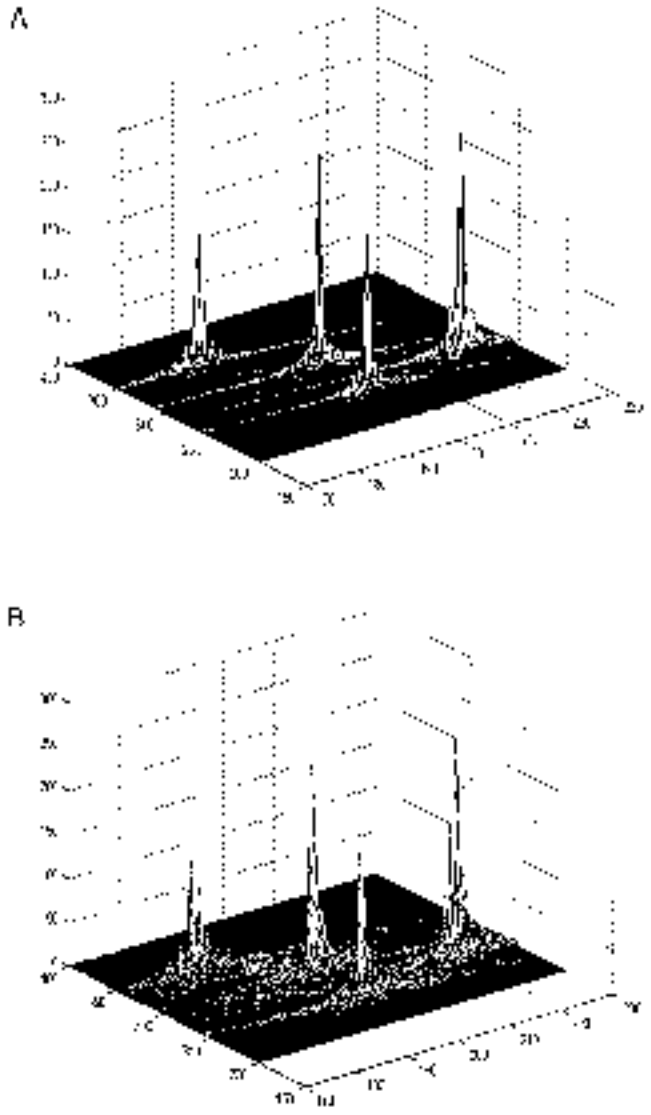

Figure 7. (a) Reconstructed SAR image ($\upsilon = 0$). (b) Reconstructed SAR image ($\upsilon = 400Km/s$).

and $\sin\tilde{\theta}_n$ and $\tilde{\tau}_n$ are defined in (25) and (26). We call this method "**Narrowband Compensation**".

We have also done simulations based on the "**Narrowband Compensation**" method. A simulation result is given in Figure 6-b, where the signal is chirp. The case used here is the same as the example discussed above for "wideband compensation" method. Figures 7-d

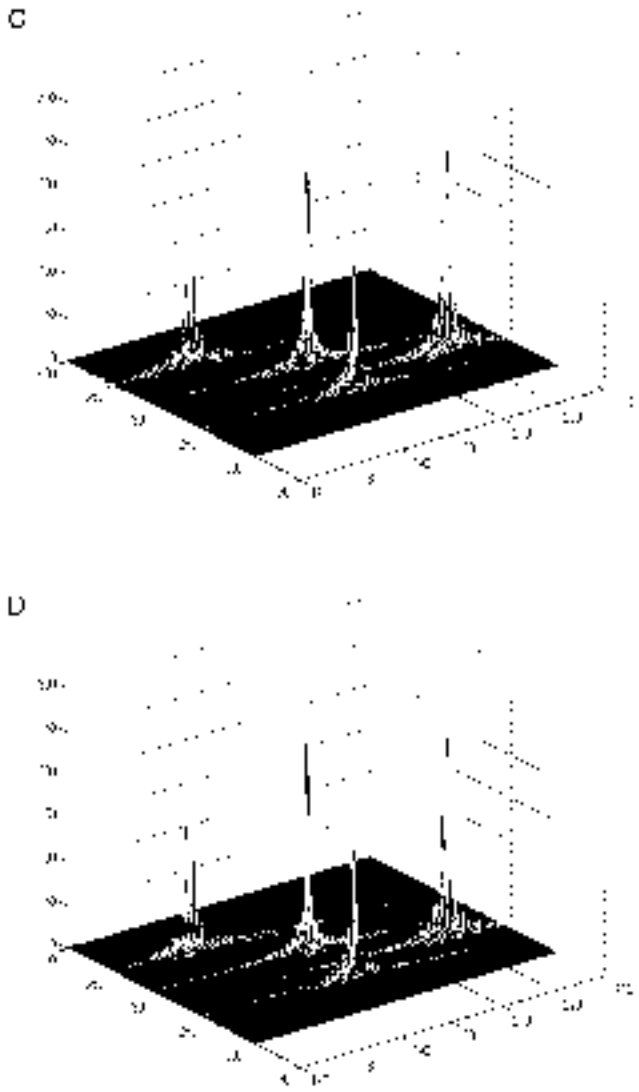

Figure 7. (c) Wideband compensation SAR image ($v = 400Km/s$). (d) Narrowband compensation SAR image ($v = 400Km/s$).

is the corresponding 3D images. For this example, the "**Narrowband Compensation**" is sufficient. But for some other examples, the "**Narrowband Compensation**" is not efficient. To save space, we will not show them here.

From the simulation, we see that for some wideband SAR signals, sometimes the "**Narrowband Compensation**" method is valid even if the narrowband condition (3)

is violated. This may be due to the fact that the dilation caused by the speed of the vehicle is different in different directions. The narrowband condition should also be changed according to different directions. Narrowband condition (3) is only the worst case.

An advantage of "**Narrowband Compensation**" over "**Wideband Compensation**" is that the "**Narrowband Compensation**" can be used for any type of signals even if the signals are non-continuous, while the "**Wideband Compensation**" requires that the signals are smooth (have at least first-order derivative). At present time, our method is only valid for a small number of separated point-targets. For large number of closely located targets, the method needs to be improved further.

5. Conclusions

It has been shown that in SAR, due to the motion of the aircraft, waveform distortion always exists. For large bandwidth and long duration SAR systems, which we believe could be the future SAR systems, waveform distortions due to moving antennas cannot be ignored. Huge amount of time and memory are needed to simulate the processing of large bandwidth and long duration SAR signals. In order to reduce the computational complexity and memory for simulation purpose, we have shown that for some kinds of signals it is correct to measure waveform distortions for very large TB with relatively small υ by reducing TB and increasing υ while keeping $TB\upsilon$ constant. Based on this observation, we are able to run simulations on SAR waveform distortions using general personal computers. The concept of wideband and narrowband process of SAR data are proposed. New method are presented for reconstructing targets using the proposed wideband and narrowband SAR model. Simulations have shown that the methods can improve the quality of the simulated SAR images.

The study is only concerned with the signal processing aspect. There are additional problems associated with large bandwidth and long duration SAR systems, such as the leakage of transmitted signals into received signals. The investigation of these problems and the search of more efficient wideband SAR processing algorithms will be our future works.

Acknowledgments

Thank the reviewers for their invaluable comments which help us to improve the paper.

Note

1. Corresponding author: Zhiping Lin, Nanyang Technological University, School of EEE, Block S2, Singapore 639798.

References

1. M. Burgos-Garcia, J. Sanmartin-Jara, F. Perez-Martiniz, and J.A. Retamosa, "Radar Sensor Using Low Probability of Interception SS-FH Signals," *IEEE AES Systems Magazine*, vol. 15, April 2000, pp. 23–28.
2. W. Carrara, R.S. Goodman, and R.M. Majewski, *Spotlight Synthetic Aperture Radar: Signal Processing Algorithms*, Artech House, 1995.
3. C. Elachi, "Space Imaging Radar in Planetary Exploration and Earth Observation," *AIAA Journal*, vol. 39, no. 4, 2001, pp. 553–563.
4. B. Huneycutt and J. Zuzek, "Frequency Use and Needs of Spaceborne Active Sensors," *International Geoscience and Remote Sensing Symposium (IGARSS)*, vol. 6, 2000, pp. 2457–2463.
5. M.G.M. Hussain, "Ultra-Wideband Impluse Radar - an Overview of the Principles," *IEEE AES Systems Magazine*, Sept. 1998, pp. 9–14.
6. Q. Jin and K.M. Wong, "The Estimation of Time Delay and Doppler Stretch of Wideband Signals," *IEEE Transactions on Signal Processing*, vol. 43, no. 4, April 1995, pp. 904–916.
7. D. Klugmann, "A Compact 94-GHz FM-CW Doppler Cloud Radar Using Semiconductor Devices for Power Generation," *Proceedings of IEEE International Conference on Geoscience and Remote Sensing Symposium (IGARSS)*, vol. 5, 2000, pp. 1801–1803.
8. X.X. Niu, P.C. Ching, and Y.T. Chan, "Wavelet Based Approach for Joint Time Delay and Doppler Stretch Measurements," *IEEE Transactions on Aerospace and Electronic Systems*, vol. 35, no. 3, July 1999, pp. 1111–1119.
9. S. Noda, K. Inomata, M. Watanabe, T. Fukae, and M. Tobioka, "A Millimeter-Wave Radar for Train Application," *Proceedings of IEEE International Conference on Vehicle Electronics Conference (IVEC)*, vol. 1, 1999, pp. 153–158.
10. J.F. Pietrasinski, T.W. Brenner, and C.J. Lesnik, "Selected Tendencies of Modern Radar and Radar Systems Development," *Proceedings of 12th International Conference on Microwave and Radar*, vol. 1, 1998, pp. 133–137.
11. A.W. Rihaczek, *Principles of High Resolution Radar*, McGraw-Hill, 1969.
12. M.I. Skolnik, *Introduction to Radar System*, 3rd ed., McGraw-Hill Higher Education, 2001.
13. M. Soumekh, *Synthetic Aperture Radar Signal Processing with MATLAB Algorithms*, John Wiley & Sons, INC. 1999.
14. J.D. Taylor, *Ultra-Wideband Radar Technology*, CRC Press, 2000.
15. B. Walker, G. Sander, M. Thompson, B. Burns, R. Fellerhoff, and D. Dubbert, A High-Resolution, Four-Band SAR Testbed with Real-Time Image Formation, http://www.sandia.gov/radar/files/igarss96.pdf.
16. L.M.H. Ulander, P.O. Frolind, and T. Martin, Processing and Calibration of Ultra-Wideband SAR Data from CARABAS-II, http://www.estec.esa.nl/ceos99/papers/p143.pdf.
17. L.G. Weiss, "Wavelets and Wideband Correlation Processing," *IEEE Signal Processing Magazine*, no. 1, Jan. 1994, pp. 13–32.
18. X.B. Yang, J.Y. Yang, and C.G. Jing, "A Research on Millimeter-Wave LFMCW Radar for Air-Field Object Imaging," *Conference Digest of International Conference on Infrared and Millimeter Waves*, 2000, pp. 413–414.
19. M.C. Zari, A.F. Zwilling, D.A. Hess, J. Jo, C.S. Anderson, and D. Chiang, "Soldier Identification System Utilizing Low Probability of Intercept (LPI) Techniques," *IEEE AES Systems Magazine*, vol. 12, July 1997, pp. 21–26.